Geochemistry of Ferrar Dolerite Sills in the Shackleton Glacier Region, Antarctica

A Senior Honors Thesis

Presented in Partial Fulfillment of the Requirements for graduation
with distinction in the Geological Sciences in the undergraduate colleges
of The Ohio State University

by

Jeffrey M. Ziga

The Ohio State University
August 2003

Project Advisor: Dr. David Elliot, Department of Geological Sciences

Dr. David Elliot
Advisor

Table of Contents

		Page
Acknowledgements		i
List of Figures and Tables		ii
Abstract		iii
Chapter		
I.	Introduction	1
II.	Regional Geology of Central Transantarctic Mountain	3
	2.1 Basement	3
	2.2 Beacon Supergroup	3
	2.3 Hanson Formation	7
III.	Ferrar Group	7
	3.1 Dating	7
	3.2 Extrusive Rocks	8
	3.3 Intrusive Rocks	8
IV.	Field Relations	10
V.	Petrography	13
VI.	Chemistry	14
	6.1 Previous Work	14
	6.2 New Data	16
VII.	Discussion	25
VIII.	Conclusion	27
List of References		28

Appendix 30

A. Petrographic Descriptions 30

Acknowledgements

I am very grateful to Dr. David H. Elliot for his guidance and support as my advisor. This paper would not have been possible without his patience and instruction.

I would also like to thank my parents for supporting me in everything I do, and for providing me with a quality education.

List of Figures and Tables

		Page
Figure 1.	Map of Antarctica showing distribution of Beacon Supergroup, Ferrar Group, other Jurassic tholeiites, and undifferentiated bedrock.	2
Figure 2.	Simplified stratigraphic section for the Beacon Supergroup in the central Transantarctic Mountains and Victoria Land	4
Figure 3.	Location and simplified geologic map for the Shackleton Glacier area, central Transantarctic Mountains.	11
Figure 4.	Diagrammatic and composite stratigraphic column for the Shackleton Glacier region, Antarctica.	12
Table 1.	Representative major and trace element analysis of Shackleton Glacier Ferrar Dolerite sill samples.	17-18
Figure 5.	Variation diagrams for major elements.	20-21
Figure 6.	Variation diagrams for trace elements.	22-24

Abstract

The Ferrar Large Igneous Province represents magmatism associated with the initial stages of Gondwana break-up during the Jurassic Period. The Ferrar Group crops out over 3000 km in a linear belt across the center of Antarctica, and includes the Ferrar Dolerite, Dufek intrusion, Kirkpatrick Basalt, and pyroclastic rocks. Sixteen samples from Ferrar Dolerite sills cropping out in the Shackleton Glacier region were analyzed to determine if olivine-bearing sills or sills with the highly evolved SPCT composition are present in the region. The analyses were also done to determine if there is evidence to support supra-crustal transport of the magma and to determine if the geographic pattern observed in lava compositions is also repeated in the sills. The sills were determined to have the common MFCT composition, but they do not exhibit the geographical pattern of compositions observed in the lavas. The absence of the SPCT and olivine-bearing compositions shows such rocks are rare. No evidence to address supra-crustal transport was found. The research expands the geographic and stratigraphic coverage of the previously limited geochemical database of the sills.

I. Introduction

The Ferrar Group represents magmatism associated with continental rifting and the breakup of Gondwana during the Jurassic Period. It crops out in a linear belt for more then 3000 km across the center of Antarctica (Fig. 1). The Ferrar includes intrusive and extrusive rocks. The intrusive components are named the Ferrar Dolerite, which is composed of diabase sills and dikes, and the Dufek intrusion, which is a layered basic intrusion. The extrusive component includes pyroclastic rocks and the Kirkpatrick Basalt lava flows. Collectively they are also referred to as the Ferrar Large Igneous Province (FLIP) (Elliot et al., 1999).

The geochemistry of the Ferrar is known mainly from analyses of lava flows. Results demonstrate a high initial Sr isotope ratio and other indicators of crustal contamination. There are two distinct lava types named the Scarab Peak Chemical Type (SPCT) and Mount Fazio Chemical Type (MFCT) (Fleming et al., 1992). The difference between the SPCT and MFCT has been described by Siders and Elliot (1985). The SPCT is a homogenous, highly evolved flow (or flows), which relative to the MFCT have low MgO, high SiO_2, and high FeO. The SPCT, the uppermost flow(s) at all known basalt outcrops, has a highly uniform composition, which has been interpreted to suggest a single source and transport over thousands of km (Elliot et al., 1999). The remaining flows form the MFCT. Lava flows, however, form less then 1% of the known volume of Ferrar rocks. The Ferrar Dolerite and the Dufek intrusion, comprising the remainder, are thought to have equal volumes, and they belong to the MFCT chemical type. Apart from a limited number of sills in Victoria Land (Hamilton, 1965; Gunn, 1966), little is known of the geochemistry of the sills.

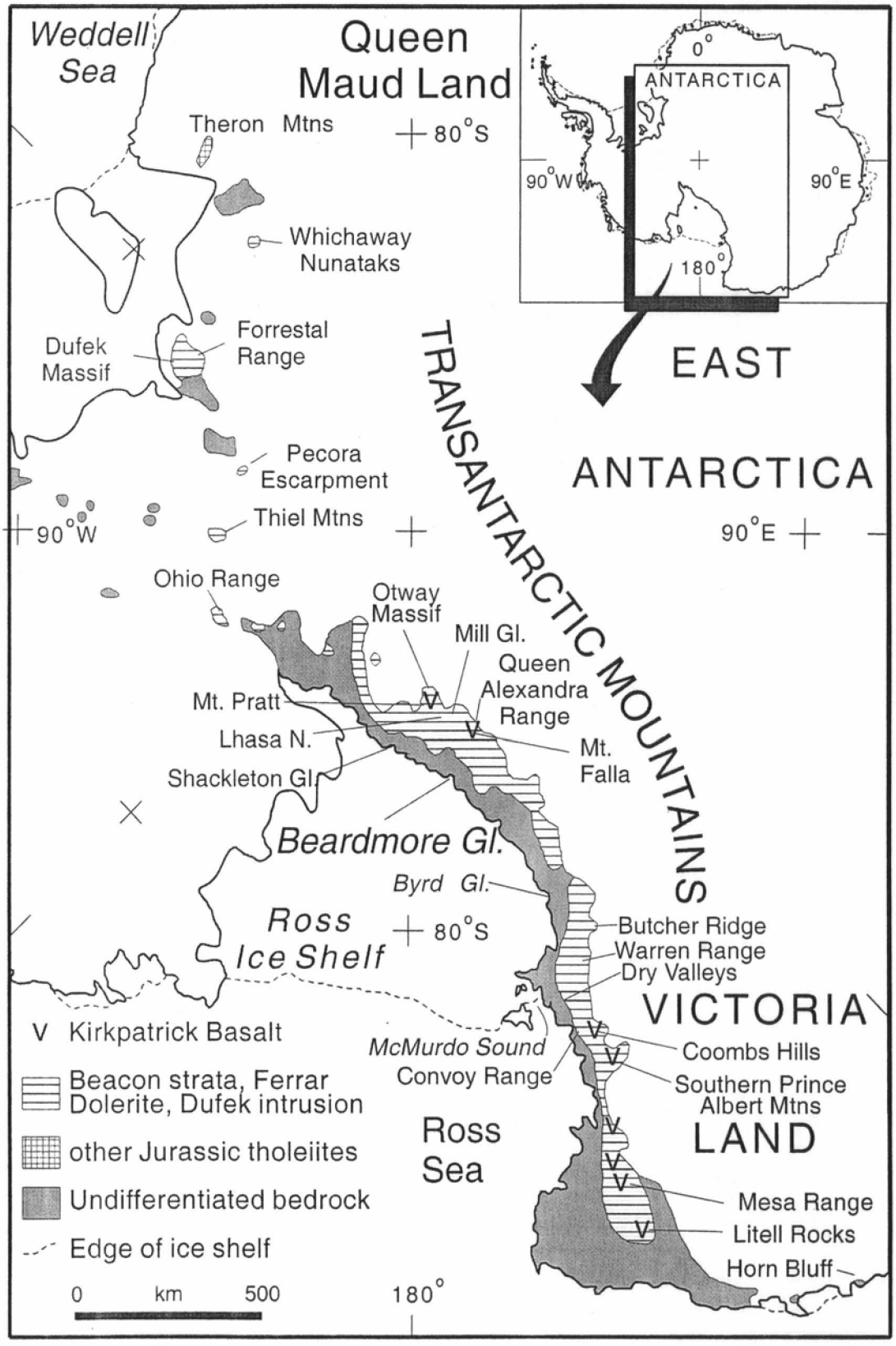

Fig. 1. Map of Antarctica showing distribution of the Beacon Supergroup, Ferrar Group, other Jurassic tholeiites, and undifferentiated bedrock.

Research reported here provides additional information on the composition of the sills, and expands on the existing limited database. The research is aimed at identifying if the SPCT composition is present in the sills, if there are additional occurrences of the mafic olivine-dolerite sills, if the geographic pattern of lava compositions is repeated in the sills, and if the sills include any information that supports supra-crustal transport of magma. This information would contribute to the understanding of the distribution of magma types in the Ferrar Group, and to their transport and emplacement.

II. Regional Geology of Central Transantarctic Mountains

Basement

The pre-Devonian basement (Collinson et al., 1994) consists of upper Proterozoic to Ordovician folded and metamorphosed sedimentary rocks and granitic batholiths. Proterozoic rocks in the central Transantarctic Mountains (CTM) are restricted to metamorphosed sedimentary rocks of the Beardmore Group and the Nimrod Group, which were affected by the Ross Orogeny of Late Cambrian-Ordovician age. The orogeny caused metamorphism and folding of the pre-existing strata along with uplift and intrusion of the Granite Harbour granitoids. The igneous and metamorphic basement is cut by a pre-Devonian regional erosion surface known as the Kukri Peneplain.

Beacon Supergroup

The Beacon Supergroup (Collinson et al., 1994) consists of relatively flat lying Devonian to Triassic sedimentary rocks that rest unconformably on pre-Devonian basement (Fig. 2). The Beacon Supergroup is important because most dolerite sills occur within it. Furthermore, the lithology of the Beacon Supergroup is of particular importance since it dictates the location of sill emplacement. In CTM (Fig. 3) the Alexandra

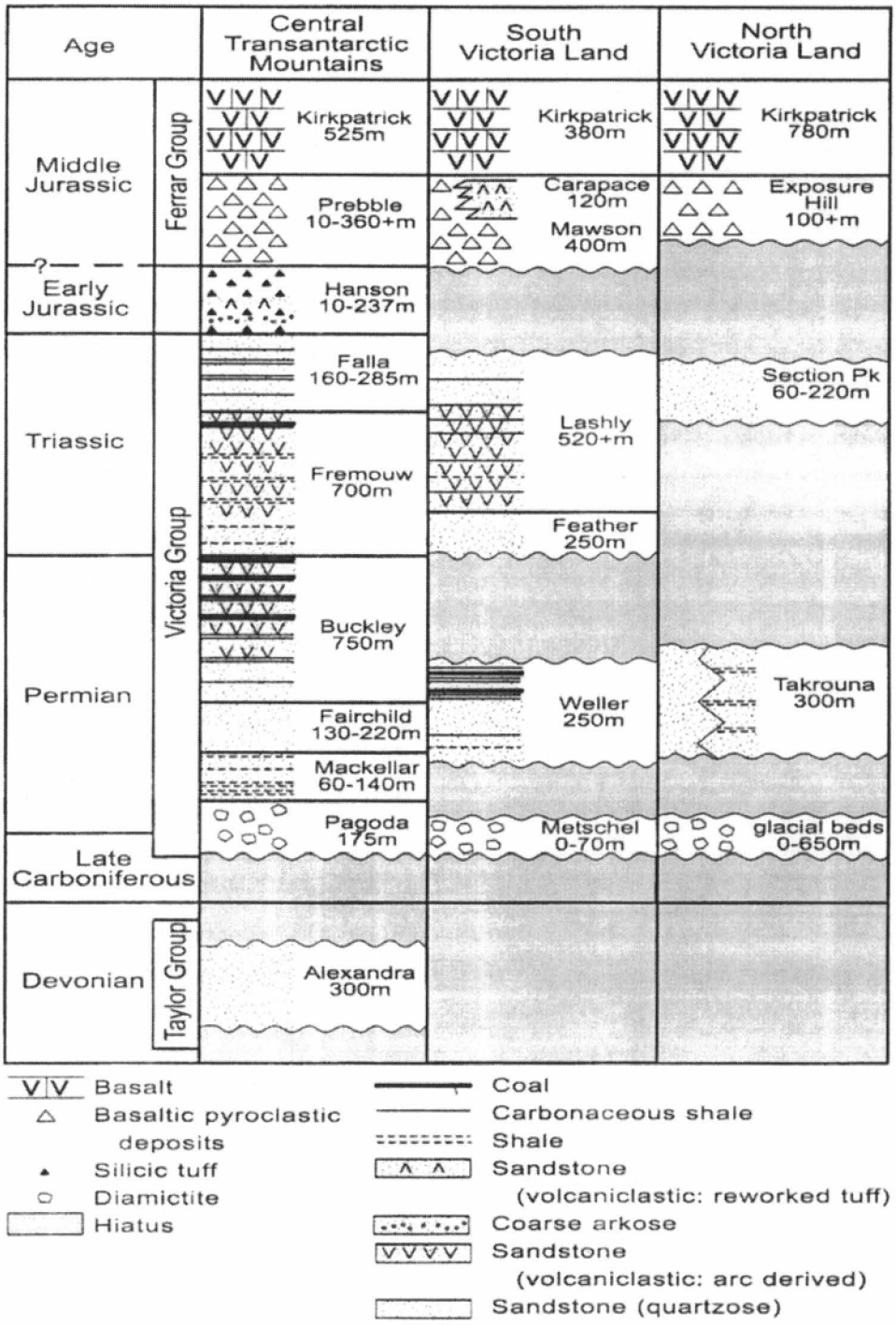

Fig. 2. Simplified stratigraphical sections for the Beacon Supergroup in the central Transantarctic Mountains and Victoria Land.

Formation is a Devonian to Carboniferous(?) quartzose sandstone unit up to 300 m thick that rests nonconformably on basement rocks. The Victoria Group disconformably overlies the Alexandra Formation. The Pagoda Formation is the basal unit of the Victoria Group and ranges between 100-200 m thick, but thins to nothing in places and also occurs as valley fill up to 395 m thick. The Pagoda Formation, Late Carboniferous to Early Permian, is a cyclic sequence of glacially-related diamictite, sandstone, and mudstone. The Mackellar Formation, Early Permian, is 60 to 150 m thick, and consists of 1 to 3 major, coarsening upward sequences of interbedded shale and fine sandstone. Multiple sandstone bodies that are upward-fining, channel-fill sandstones cap these larger, coarsening upward sequences. The Fairchild Formation, which is Early Permian as well, is a thick medium to coarse-grained sandstone unit. The unit is mostly interconnected channel-form sandstone sheets that are 5 to 20 m thick and tens to hundreds of meters wide. The thickness of the formation varies from 130-230 m. The Buckley Formation overlies the Fairchild, and is divided into distinct lower and upper parts. The lower Buckley is late Early Permian. It is a cyclic sequence of sandstone, carbonaceous siltstone/mudstone, and coal. The base of the sequence, everywhere it is exposed, consists of lenticular beds of a well-rounded, quartz pebble conglomerate that are overlain by coal measures. The coal measures are 70% sandstone sheet-like bodies 10 to 20 m thick and 2 to over 10 km wide, with the other 30% being floodplain deposits of siltstone/mudstone and coal. The thickness of the unit is approximately 300 m. The upper Buckley is Late Permian in age, and is approximately 400 m thick. It consists of approximately equal proportions of resistant course to medium-grained sandstone, and less resistant fine sandstone, siltstone, mudstone and coal. The coarser units are made up

of 1 to 10 fining upward sequences that are from 1 to 5 m thick. These sequences contain mudstone within the sandstone bodies and some have mudstone at the top of the sequence. Each unit extends laterally for tens to hundreds of meters. The less resistant units are dominantly carbonaceous siltstone and mudstone. The upper parts of the finer grained units commonly contain coal beds from 0.1 to 10 m thick, and also thinly bedded sheets of fine to medium grained sandstone. The Fremouw overlies the Buckley and is divided into three parts. The lower and middle Fremouw are quite similar, and both are Early Triassic. The sandstone units in the lower member are coarse to medium-grained and form channel-form sheets that extend laterally for hundreds of meters. Fine grained floodplain deposits form about half the lower Fremouw, and are composed of greenish gray siltstone and mudstone. The middle Fremouw is distinguished by having a higher proportion of finer-grained floodplain deposits to coarse-grained channel deposits. In the middle member sandstone bodies are less sheet-like and only extend for tens of meters before pinching out; fine grained siltstone and mudstone dominate. The two members combined are up to 330 m thick. The lower part of the upper Fremouw is Middle Triassic, but the top 100 m is Late Triassic. The member has a total thickness of 220 m. It forms extensive resistant slopes of light gray medium to fine grained sandstone. The basal 30 m form a series of resistant ledges. Above this platform are thick sandstone units up to 100 m thick that are separated by thin fine-grained siltstone and mudstone units. The Falla Formation (Collinson et al., 1994; Elliot, 1996) is the uppermost unit in the Beacon Supergroup, and is Late Triassic in age. It is up to 296 m thick and composed of fining upward cycles of course to fine grained sandstone capped by carbonaceous shale and occasional thin coal seams.

Hanson Formation

The Hanson Formation (Elliot, 1996; Elliot, 2000) is a Lower Jurassic tuffaceous and volcaniclastic sequence that rests disconformably on the underlying Falla Formation. It ranges from 10 to 238 m thick. The greatest thickness occurs at its type section at Mount Falla where it is divided into three informal members. The lower member is 69 m thick and is composed of weakly bedded green tuffaceous sandstones, and cross stratified quartzose sandstones that grade up into volcaniclastic sandstone. The middle member is 69.5 m thick, and is composed of resistant tuffs with minor amounts of interbedded volcaniclastic sandstone. The upper member is a 99.5 m thick slope-forming tuff and reworked tuff sequence. This threefold division is not evident at other locations, but the uppermost beds are invariably dominated by tuffs.

III. Ferrar Group

Dating

Reliable age determinations for the Ferrar Large Igneous Province have been hard to obtain due to non-ideal behavior of K-Ar and Rb-Sr isotopic systems resulting from low temperature alteration during the Cretaceous (Fleming et al., 1995). Heimann et al. (1994) showed that the magmatism occurred at 176.6 +/- 1.8 Ma by analyzing feldspar separates, derived from lava flows and pyroclastic rocks underlying the lavas, using the $^{40}Ar/^{39}Ar$ incremental heating method. Fleming et al. (1997) used the same methods as Heimann et al. (1994) to date the intrusive Ferrar Dolerite and obtained an age of 176.7 +/- 0.6 Ma, which is identical to the interpreted age of the extrusive rocks. Heimann et al. (1994) also indicated that the ages of the pyroclastic rocks and the Kirkpatrick basalt are essentially identical over large distances (1200 km) in CTM, SVL, and NVL. Both

Heimann et al. (1994) and Fleming et al. (1997) inferred that the emplacement of both intrusive and extrusive rocks occurred in 1 my or less.

Extrusive Rocks

The extrusive component of the Ferrar Group comprises pyroclastic rocks overlain by basalt flows. The Prebble Formation (Elliot & Larsen, 1993; Elliot, 2000), the name of the pyroclastic unit in the CTM, is between 10 and 360+ m. It is composed mostly of tuff-breccias with lesser amounts of lapillistone, lapilli-tuff, and tuff. The underlying contact appears conformable, but a disconformity is inferred from the Hanson Formation regional stratigraphy (Elliot, 1996).

The Kirkpatrick Basalt (Elliot, 1970) is a continental flood basalt that in CTM crops out in the region of the Beardmore Glacier, and has an extant outcrop of approximately 110 km^2. The Kirkpatrick Basalt rests without angular discordance on the Prebble Formation, but some paleotopography was present at the time of eruption as shown by lavas lapping onto a volcanic cone belonging to the Prebble Formation. The Kirkpatrick Basalt is the uppermost unit wherever exposed and its thickness thus varies greatly. The thickest section in CTM occurs at Storm Peak where 13 flows are present that have a total thickness of 525 m; flows have thicknesses ranging from 11 to 135 m. Exceptionally thick flows (50+ m) are most likely the result of ponding of lava by topography.

Intrusive Rocks

The intrusive bodies (Elliot & Fleming, in press) include the Dufek layered basic intrusion and the Ferrar Dolerite. The Dufek layered basic intrusion crops out in two ranges (Dufek Massif and Forrestal Range) that are 40+ km apart. The combined areal

extent of the two intrusions is 6600 km^2 with a combined estimated volume of $6x10^4$ km^3 (Elliot & Fleming, in press). The Ferrar Dolerite forms massive bodies, dikes, and sills up to 700 m thick. The maximum outcrop width of Ferrar rocks in CTM is approximately 160 km. The truncation of the sills at the Transantarctic Mountains (TAM) front suggests that they originally extended farther toward the paleo-Pacific margin (Fig. 1). Based on geophysical data, Ferrar rocks are also interpreted to extend about 100 km onto the Precambrian craton below the ice cover.

Several massive bodies crop out throughout the TAM. In CTM much of Lhasa Nunatak and the southern part of the Supporters Range in the Mill Glacier region are formed of large amounts of dolerite. Other massive bodies are present in the Convoy Range, Coombs Hills, and the Warren Range. A large mafic body underlies the Butcher Ridge Igneous complex, has an areal extent of 3000 km^2, and a minimum thickness of 2 km (Elliot & Fleming, in press).

Sills make up the vast majority of the Ferrar Dolerite, and the sills are thought to be volumetrically equivalent to the Dufek intrusion. The sills intrude the pre-Devonian basement in only a few places including Thanksgiving Point at the Shackleton Glacier. Most of the sills intrude the Beacon Supergroup, and the extent of sill outcrop is largely coincident with Beacon outcrop. A few sills intrude pyroclastic rocks at Otway Massif and Mount Pratt in the CTM. There is no documented occurrence of a sill intruding the lava flows. The thickness of the sills averages between 100 and 200 m, but thicknesses of 700+ m are found in the Dry Valleys region. In general the sills are bedding parallel or slightly discordant lower in the section. However, sills become complex and more erratic at higher stratigraphic levels. Sills have been observed to change stratigraphic position by

as much as 100 m over several hundred meters. Sills have also been observed to ramp from one stratigraphic level to another, or to end in thin dikes that connect to a sill of similar thickness at another stratigraphic level; sills may also branch or cross, or form composite sills (two sills in contact). The areal extent of individual sills is difficult to determine since most cannot be positively identified from one outcrop to another due to the previously described geometry and uniform geochemistry (see chemistry). The Basement Sill in Victoria Land has an estimated areal extent of 5,000 km^2, and has an outcrop length of 150 km. The Peneplain Sill has an estimated areal extent of 6,000 km^2 (Elliot & Fleming, in press).

Dikes are numerous, but are volumetrically insignificant. Most dikes have thicknesses in the range from 0.2 to 3 m, extend for only a few kilometers in outcrop, and are commonly segmented. Massive feeder dikes and dike swarms have not been found, and very few massive dikes have been reported. A dike in the Dry Valleys is 50 m thick but may be an inclined sheet ramping between sills. Plug-like bodies, interpreted to be feeder systems for volcanoes, range from 10 to 100+ m in diameter (Elliot & Fleming, in press).

IV. Field Relations

Samples from sixteen sills in Shackleton Glacier region in the CTM were analyzed. The samples were collected by David H. Elliot during the 1995-96 field season. Locations of the samples are indicated in Figure 3, and their approximate stratigraphic positions are shown in Figure 4. The only sample analyzed that was emplaced into the pre-Devonian basement is from Thanksgiving Point. Most of the samples analyzed come from sills intruded into the Victoria Group. The samples collected at Rougier Hill come

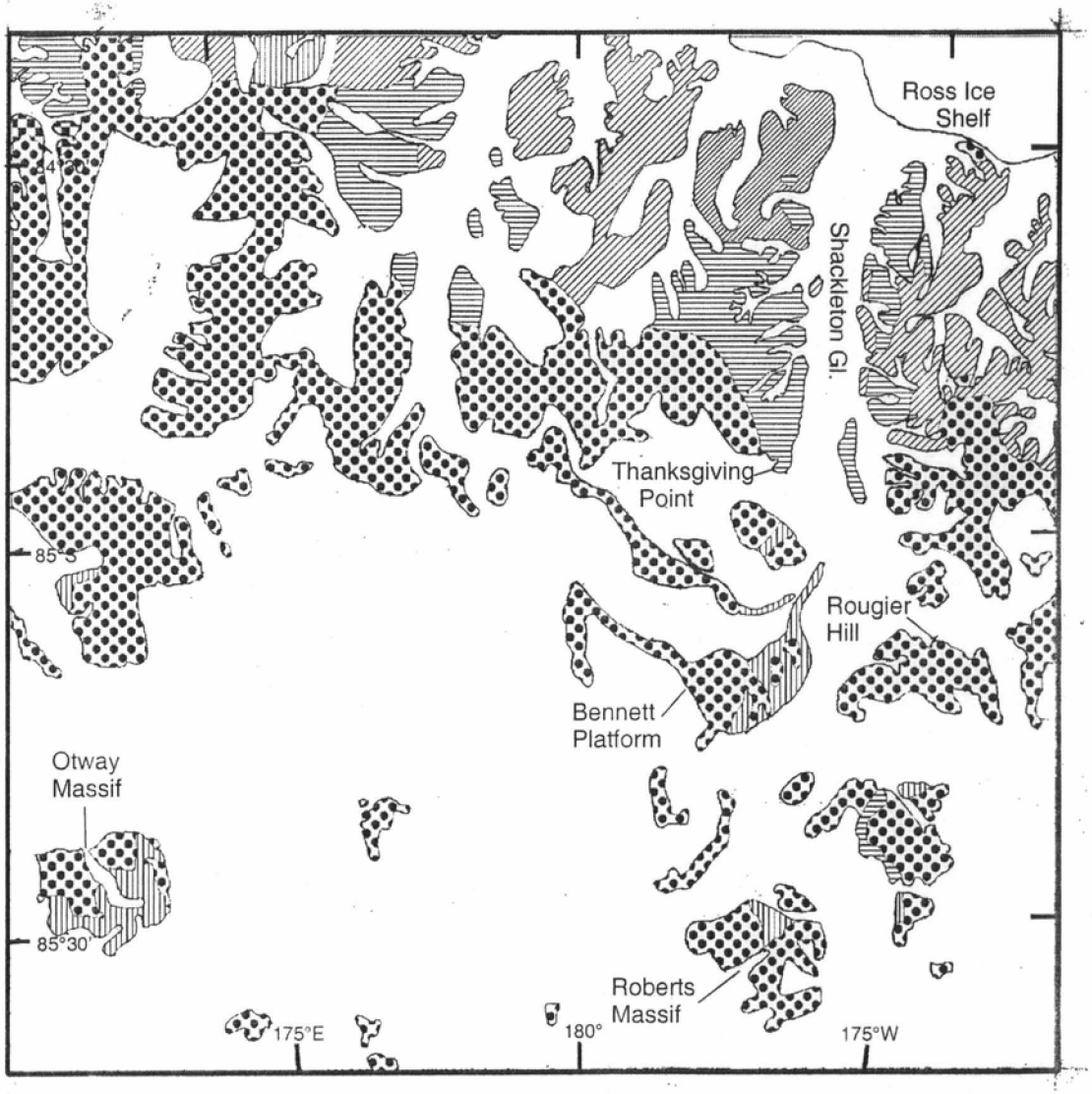

Fig. 3. Location and simplified geologic map for the Shackleton Glacier area, central Transantarctic Mountains.

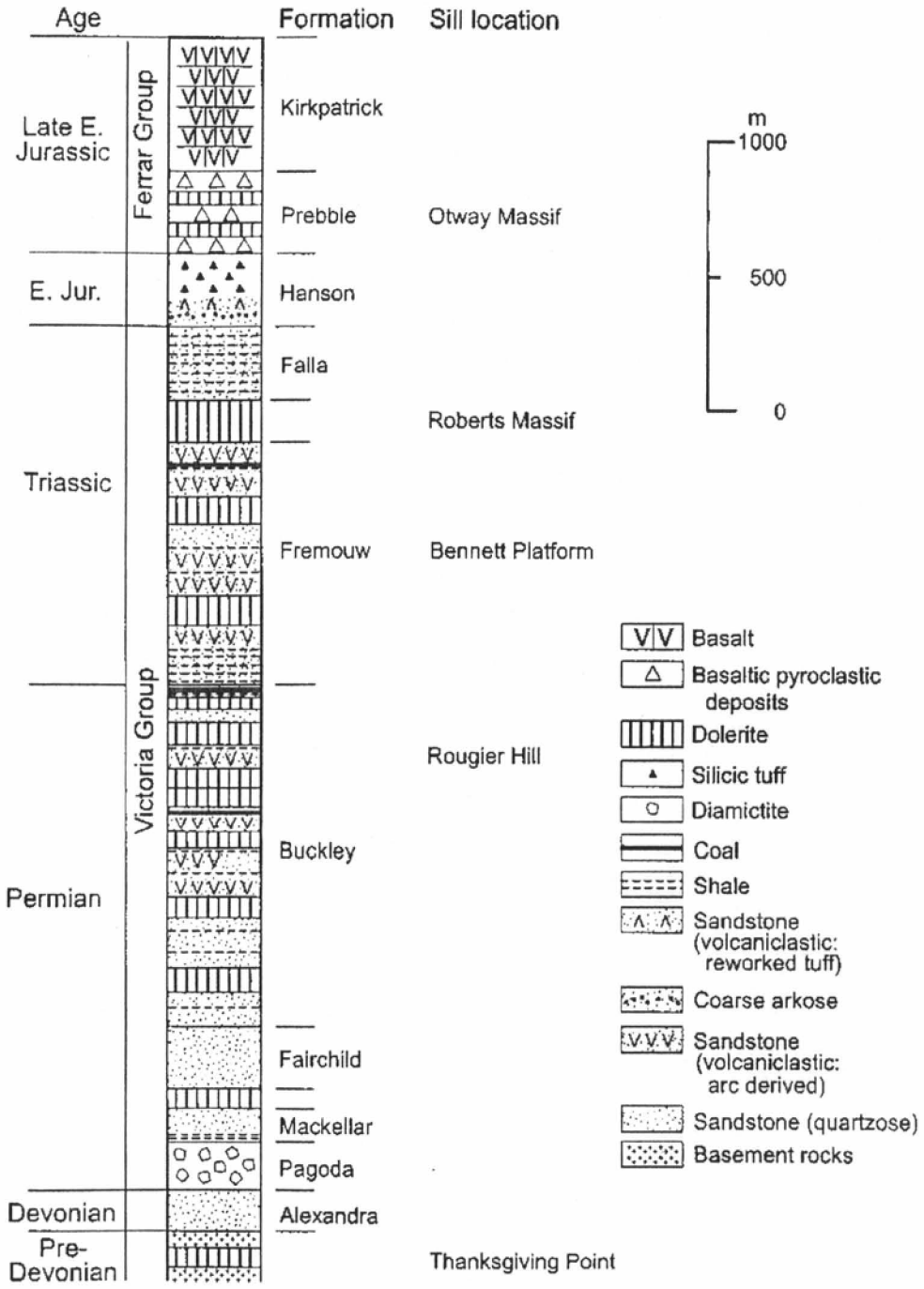

Fig. 4. Diagrammatic and composite stratigraphic column for the Shackleton Glacier region, Antarctica.

from five sills that intrude the Permian upper Buckley Formation. The samples collected from Bennett Platform come from three sills that intrude the Triassic Fremouw Formation. The samples from Roberts Massif come from two sills that intrude the contact between the Fremouw and Falla Formations. The samples from Otway Massif come from various sills that intrude the Prebble Formation of the Ferrar Group. All analyzed samples come from the chilled margin or close to the chilled margin of the sill.

In the Shackleton Glacier region, as in other parts of the TAM, sills appear to be preferentially emplaced at stratigraphic contacts with marked lithologic contrasts, for instance at the Mackellar/Fairchild contact. Furthermore, sills are more abundant in the mudstone and shale-rich upper Buckley Formation. Permian strata also contains more sills than the Triassic strata.

V. Petrography

In thin section the rocks are dominantly composed of plagioclase and pyroxene in subophitic to intergranular textures. The plagioclase forms phenocrysts in the coarser grained rocks, forms much of the matrix in the finer grained rocks, and forms thin wisp like crystals and skeletal laths where enclosed in glass. The most common pyroxene is augite with pigeonite being secondary in most samples. Orthopyroxene occurs in one sample as xenocrysts (96-51-76), but also occurs as a primary mineral (96-51-18, 96-73-6). The rocks also contain, in lesser amounts, granophyric intergrowths, sanidine, quartz, apatite, glass, and opaques. Granophyric intergrowths are composed of quartz and alkali feldspar and are relatively minor in most rocks, but in one rock (96-64-9) abundant intergrowths are present (this sample is discussed later). Sanidine has been found in only one sample (96-51-18). Identifiable quartz crystals form a very minor component in a few

rocks. Apatite forms small needles in the matrix of nearly all the samples. A glassy or quenched matrix is uncommon and occurs in only two samples (96-64-1 and 96-64-14). Opaques occur mainly as small phenocrysts, but also as disseminated grains throughout the matrix.

The samples have undergone slight to moderate alteration. The most prevalent form is the alteration of pyroxenes to a brown fibrous mineral that is interpreted to be tremolite/actinolite. Plagioclase and quartzofeldspathic mesostasis, in some cases, are altered to an orange-brown phyllosilicate. The glassy matrix is also slightly altered to a yellow mineraloid (palagonite).

The unique sample (96-64-9) has a much smaller proportion of pyroxenes relative to quartzofeldspathic minerals than the other samples. The majority of the rock consists of quartzofeldspathic intergrowths and granophyre. The sample also exhibits thin elongate plagioclase crystals and rod shaped opaques, which indicate high fluid (water) content of the crystallizing melt. Alteration is moderate to strong with a dark pleochroic phyllosilicate (biotite?) occurring as an alteration product.

VI. Chemistry

Previous Work

Most of the previous work done on the geochemistry of the Ferrar comes from lava flows (Siders & Elliot, 1985; Elliot et al., 1995; Fleming et al., 1992, 1995). The Ferrar rocks are characterized by high initial $^{87}Sr/^{86}Sr$ isotope ratios that are more like those of continental crust than of upper mantle. These high initial $^{87}Sr/^{86}Sr$ ratios suggested two alternative hypotheses for the origin and evolution of Ferrar magmas. The hypothesis promoted by Faure et al. (1982) suggested that the magmas were mantle-

derived and the high initial $^{87}Sr/^{86}Sr$ ratios and their correlation with major elements reflected crustal assimilation. The other hypothesis proposed that the magma originated in mantle with enriched $^{87}Sr/^{86}Sr$ isotope ratios and that the chemical variations arose from fractional crystallization accompanied by minor assimilation (Kyle, 1980). Hoefs et al. (1980) found a positive correlation between O isotopes and high initial $^{87}Sr/^{86}Sr$ ratios for lavas in the CTM and attributed this to crustal contamination. However, Kyle et al. (1983) reported a weak correlation between O isotopes and high initial $^{87}Sr/^{86}Sr$ in SVL lavas, which they argued did not indicate crustal assimilation. Both hypotheses have problems that arise mainly from the high initial $^{87}Sr/^{86}Sr$ ratios. Fleming et al. (1992) showed that the high initial $^{87}Sr/^{86}Sr$ ratio is not relevant to discussion of the origin of the magmas since the original $^{87}Sr/^{86}Sr$ ratio was changed by alteration events in the Cretaceous. Further, Fleming et al. (1995) argued that for understanding the origin of the magmas, $^{146}Nd/^{144}Nd$ isotope ratios are more significant due to immobility of Rare Earth Elements (REE), which makes them more resistant to alteration than $^{87}Sr/^{86}Sr$ ratios. Fractionation is clearly the most important factor in the evolution of the Ferrar magmas as demonstrated by the good correlation between indices of fractionation (Mg number [Mg/(Mg+Fe)] and SiO_2) and major and trace element concentrations (Haban, 1984). Nevertheless, Fleming et al. (1995) demonstrated, using $^{146}Nd/^{144}Nd$ ratios, that assimilation did play a role, albeit a rather insignificant one, and determined that less than 5% crustal material was introduced into the melt by mass assimilation (after initial upper crustal evolution).

Little geochemical work has been done on the Ferrar Dolerite since the original studies by Hamilton (1965), Gunn (1966), and Compston et al. (1968). Although,

subsequent work has been undertaken by many researchers, the number of sill samples analyzed is relatively small compared to the flows (Haban, 1984; Hergt et al., 1989; Brewer et al., 1992; Brotzu et al., 1992; Fleming et al., 1995; and Elliot et al., 1995). SPCT sills have been reported only in the Theron Mountains and Whichaway Nunataks (Leat et al., in press), which are 1300 km distant toward the inferred source region for the Ferrar magmas. All analyzed sills belong to the MFCT. The sills are characterized by a distinct crustal imprint in trace element patterns and initial isotope ratios. Like the MFCT lavas, the sills (compared to mid ocean ridge basalts [MORB]) have elevated SiO_2 and low TiO_2 and P_2O_5 contents. The trace elements (compared to MORB) show relative enrichment in large ion lithophile (LIL) elements relative to high field strength (HFS) elements, strong negative Eu anomalies, and the light REE exhibit a steep slope and heavy REE have a relatively flat slope on chondrite normalized patterns (Fleming et al., 1995). In these respects the Ferrar Group is like many other continental flood basalt provinces [Parana (Peate, 1997), Karoo (Marsh et al., 1997), and Columbia River (Hooper, 1997)].

New Data

Sixteen samples were analyzed for major and trace element abundances (Table 1). Major and trace element data were collected using X-ray fluorescence techniques as described by Fleming et al. (1992). The sills show a range of compositions and are moderately to highly evolved (MgO = 7.5-2.8%; Mg number = 65.4-44.8). The data lie in the MFCT range of compositions with one sample having anomalous chemistry. The data were plotted against Mg number since it is a good indicator of magma evolution in a tholeiitic melt fractionating plagioclase and pyroxenes. Of the major elements SiO_2, TiO_2,

Table 1. Representative Major and Trace Element Analyses of Shackleton Glacier Ferrar Dolerite Sill Samples.

Sample	96-50-5	96-51-18	96-51-41	96-51-42	96-51-72	96-51-76	96-57-4	96-64-1
SiO_2	55.19	55.58	54.04	53.71	54.72	56.28	55.16	55.46
Al_2O_3	14.88	15.02	16.51	16.37	15.17	15.19	14.85	14.83
TiO_2	0.609	0.632	0.495	0.505	0.621	0.800	0.643	0.866
Fe_2O_3	1.17	1.16	1.05	1.06	1.18	1.22	1.21	1.34
FeO[a]	7.80	7.74	6.98	7.10	7.85	8.16	8.05	8.96
MnO	0.167	0.166	0.144	0.146	0.175	0.163	0.163	0.178
MgO	6.59	6.29	7.40	7.51	6.96	5.44	6.72	5.32
CaO	10.93	10.50	10.94	11.57	10.76	9.74	10.31	10.13
Na_2O	1.86	2.00	1.87	1.81	1.79	2.05	2.01	2.02
K_2O	0.71	0.83	0.50	0.14	0.68	0.82	0.79	0.77
P_2O_5	0.091	0.098	0.086	0.080	0.091	0.128	0.098	0.117
Total	100.00	100.00	100.00	100.00	99.91	100.00	100.00	100.00
LOI	0.64	0.65	1.12	1.43	1.82	1.29	1.52	1.12
Total[b]	99.62	100.15	99.90	99.44	100.31	100.03	99.50	100.26
Mg no.[c]	60.59	59.65	65.88	65.82	61.74	54.82	60.32	51.97
ppm								
V	227	250	171	205	204	228	274	284
Cr	133	113	251	271	150	148	124	56
Ni	78	72	156	152	84	72	83	52
Cu	140	148	84	87	142	105	112	208
Zn	104	111	69	70	109	93	89	145
As	<3	<3	<3	7	<3	3	<3	<3
Rb	27	30	19	3	25	27	30	74
Sr	119	124	121	128	122	138	140	140
Y	21	21	17	18	21	26	21	26
Zr	90	92	66	67	88	127	90	114
Nb	6	7	6	6	6	8	7	7
Mo	<1	<1	<1	<1	<1	<1	<1	<1
Ba	197	230	158	82	197	252	212	254
Pb	12	11	8	8	11	12	15	12
Th	5	6	3	4	3	4	5	5
U	2	3	2	<2	3	2	2	3

Table 1. (continued)

Sample	96-64-9	96-64-13	96-64-14	96-73-6	96-73-10	96-73-16	96-74-2	96-74-7
SiO_2	65.67	56.35	55.50	54.70	54.87	56.91	57.24	54.10
Al_2O_3	14.15	13.97	14.65	15.77	15.30	13.83	13.92	16.79
TiO_2	0.783	0.976	1.004	0.549	0.637	1.134	1.144	0.650
Fe_2O_3	0.92	1.42	1.41	1.06	1.19	1.44	1.43	1.10
FeO[a]	6.10	9.49	9.41	7.06	7.93	9.63	9.55	7.32
MnO	0.125	0.182	0.180	0.147	0.167	0.180	0.165	0.152
MgO	2.78	4.95	4.95	7.12	6.59	4.40	4.50	6.31
CaO	4.64	9.20	10.02	11.04	11.00	9.11	8.27	10.81
Na_2O	2.36	2.14	1.97	1.90	1.87	2.19	2.34	1.92
K_2O	2.35	1.19	0.78	0.56	0.36	1.03	1.29	0.76
P_2O_5	0.121	0.137	0.124	0.096	0.095	0.148	0.148	0.095
Total	100.00	100.00	100.00	100.00	100.00	100.00	100.00	100.00
LOI	2.02	1.13	0.83	0.88	1.30	0.76	1.36	0.89
Total[b]	100.25	99.91	100.21	100.20	99.76	99.87	99.62	99.04
Mg no.[c]	44.83	48.71	48.91	64.73	60.20	45.42	46.14	61.05
ppm								
V	114	281	301	205	248	295	313	212
Cr	77	47	56	263	156	45	44	137
Ni	34	46	50	123	78	42	43	81
Cu	86	107	110	117	136	118	111	103
Zn	103	99	98	89	103	106	103	78
As	<3	<3	<3	<3	<3	<3	3	<3
Rb	105	46	44	20	12	34	52	29
Sr	149	134	151	138	126	135	133	128
Y	34	30	28	17	22	32	32	21
Zr	193	130	122	72	95	147	148	90
Nb	13	8	8	7	7	9	9	7
Mo	<1	<1	<1	<1	<1	<1	<1	<1
Ba	494	301	273	175	130	288	304	204
Pb	21	13	12	8	13	16	11	10
Th	10	6	5	2	4	7	6	2
U	3	2	2	<2	<2	2	3	2

All data computed by XRF analysis at New Mexico Institute of Mining and Technology, courtesy of P.R. Kyle.

[a] *Major element oxides normalized to 100% with $Fe_2O_3/FeO = 0.15$.*

[b] *Total: original analytical total before normalization to 100%.*

[c] *Mg no.: Mg-number ($Mg/(Mg + Fe^{2+})$).*

FeO, Na_2O, K_2O, and P_2O_5 have a positive correlation with Mg number (Fig. 5). Al_2O_3 and CaO have a negative correlation with Mg number (Fig. 5). The major element trends represent the early crystallization of Ca-rich plagioclase and clinopyroxenes in a fractionating melt. Of the trace elements, Th, Zr, Nb, Rb, Ba, Pb, Y, and V all increase as the magma evolves (Fig. 6). Th, Zr, Y, and Nb are high field strength elements and strongly incompatible, and their abundances should increase as the melt evolves by fractionation since they do not substitute for other elements in fractionating mineral phases (plagioclase, pyroxenes, and iron oxides). Rb, Ba, and Pb are LIL elements that substitute for K (respective average partition coefficients: 0.38, 6.6, 1.0) in minerals crystallizing in the late stages of magma evolution; K, Rb, and Pb exhibit significant scatter that may be attributed to secondary alteration. Cr and Ni both decrease, with good fits as evolution of the magma progresses. This decrease is expected since Cr and Ni substitute readily for Mg and Fe in clinopyroxene and olivine, respectively; because olivine did not crystallize out of the magma, Ni must be substituting in clinopyroxene (partition coefficient: Cr=8.4 and Ni=2.6). Sr shows significant scatter, but overall little change during fractionation. The scatter exhibited by the Sr is attributable to alteration during the Cretaceous as described by Fleming et al. (1992, 1999), and the small change in abundance with magma evolution to a partition coefficient close to 1 (Fleming et al., 1995). The trends of the major and trace elements are those expected for the evolution of a magma that is dominated by fractional crystallization.

The anomalous sample (96-64-9) does not correspond with the trends observed for all other samples. The sample is characterized by a moderate Mg-number (44.8) with

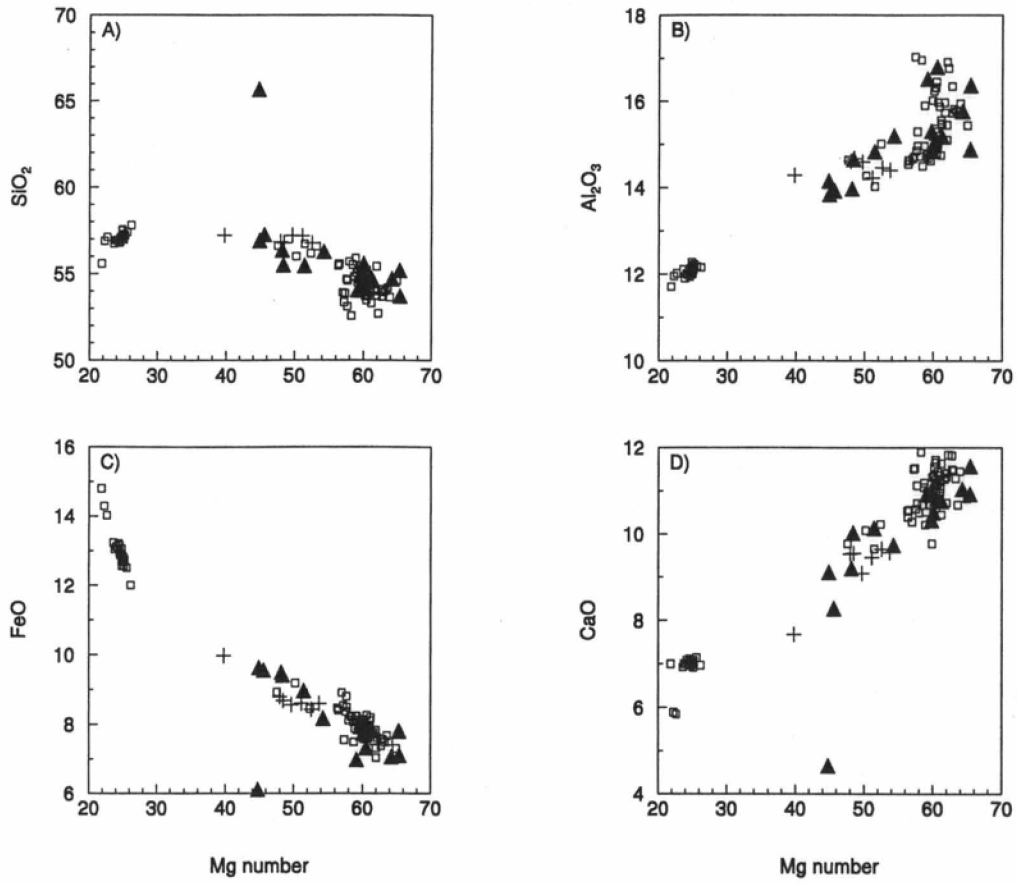

Fig. 5. Variation diagrams for major elements (oxides in weight percent) against Mg-number (Mg/(Mg+Fe^{2+})for MFCT and SPCT rocks. Symbols: squares, lavas; crosses, previous sill data; triangles, new sill data. The cluster of points between Mg-number 20 and 30 represents SPCT composition. Mg-number decreases with increasing magma evolution. (Siders, 1983; Elliot et al., 1995)

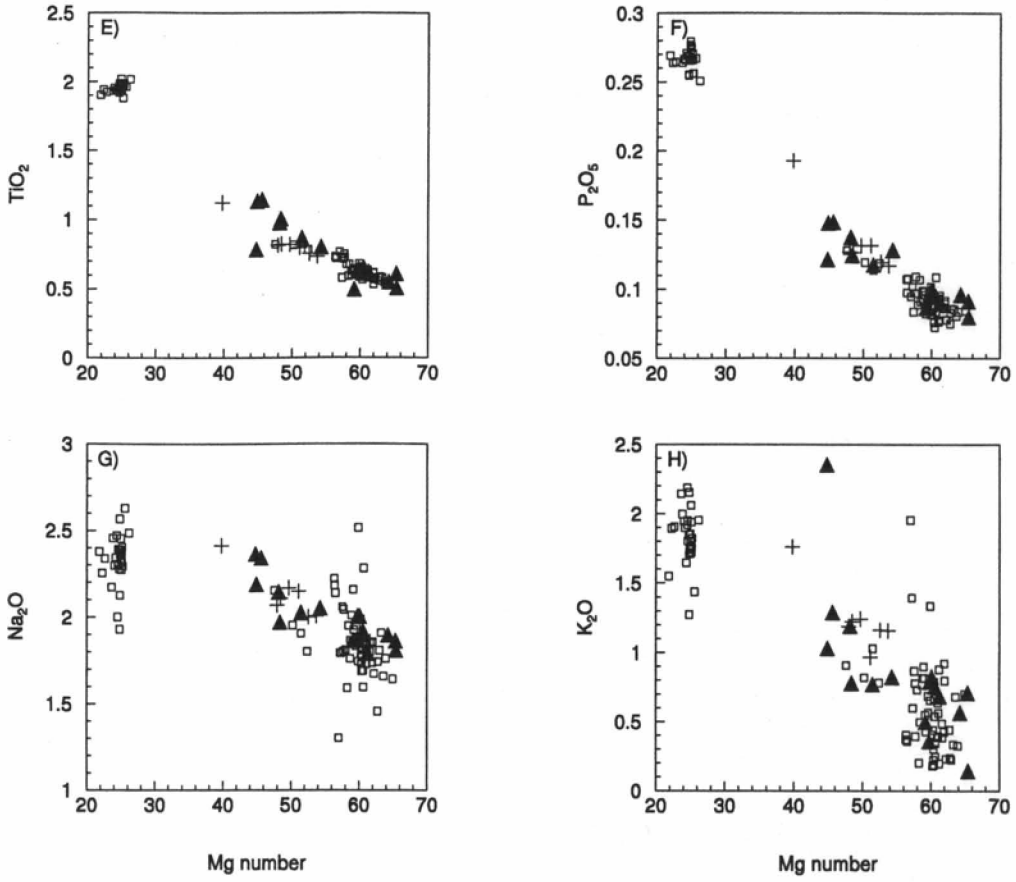

Fig. 5. (continued)

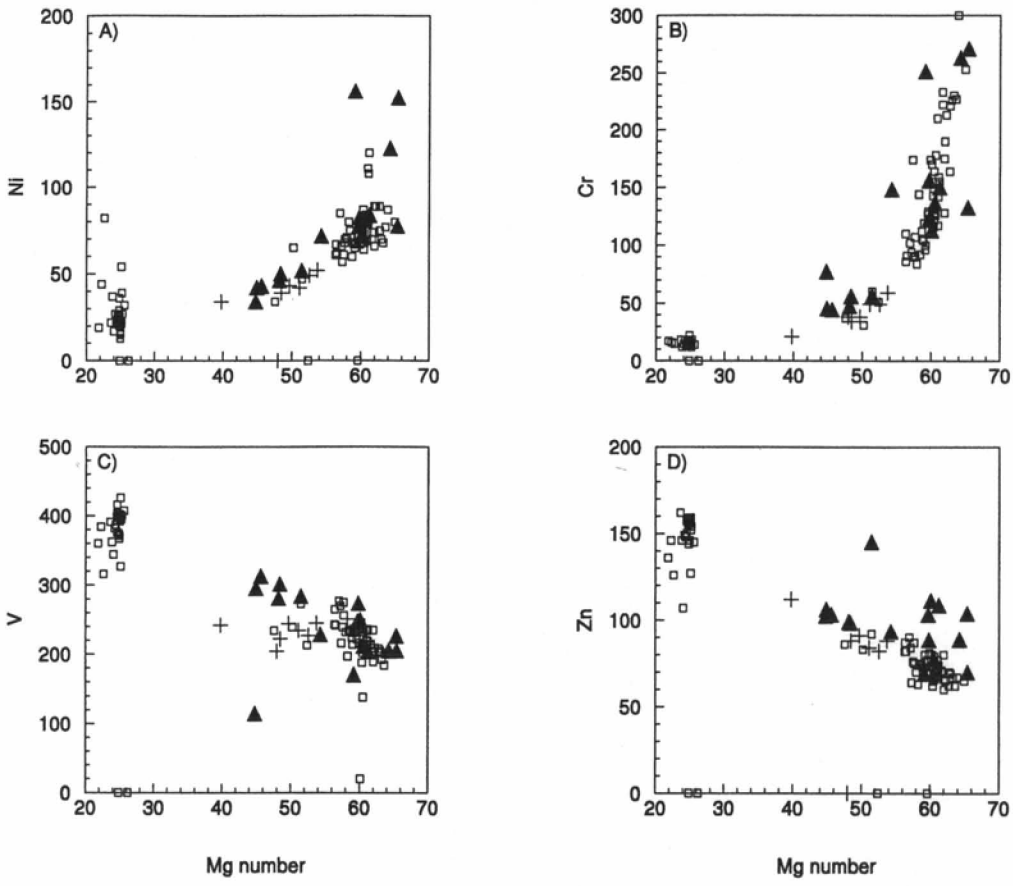

Fig. 6. Variation diagrams for selected trace elements (in ppm) against Mg-number ($Mg/(Mg+Fe^{2+})$ for MFCT and SPCT rocks. Symbols as for Figure 5.

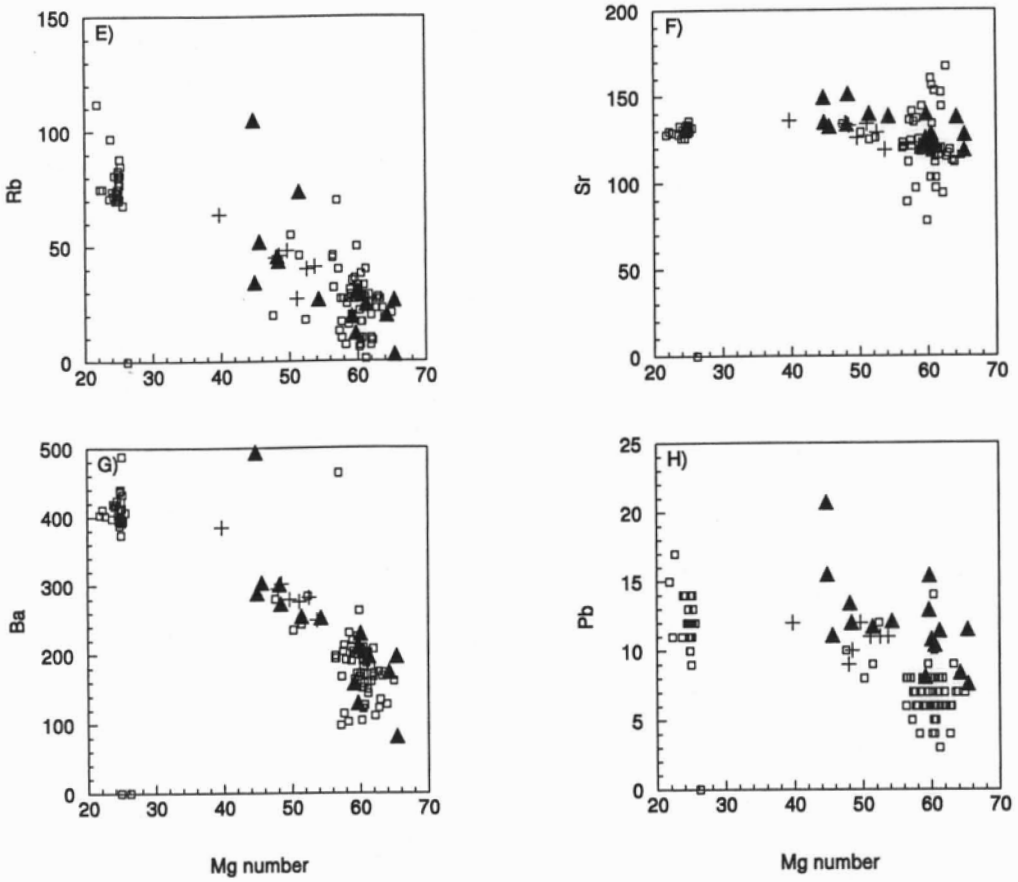

Fig. 6. (continued)

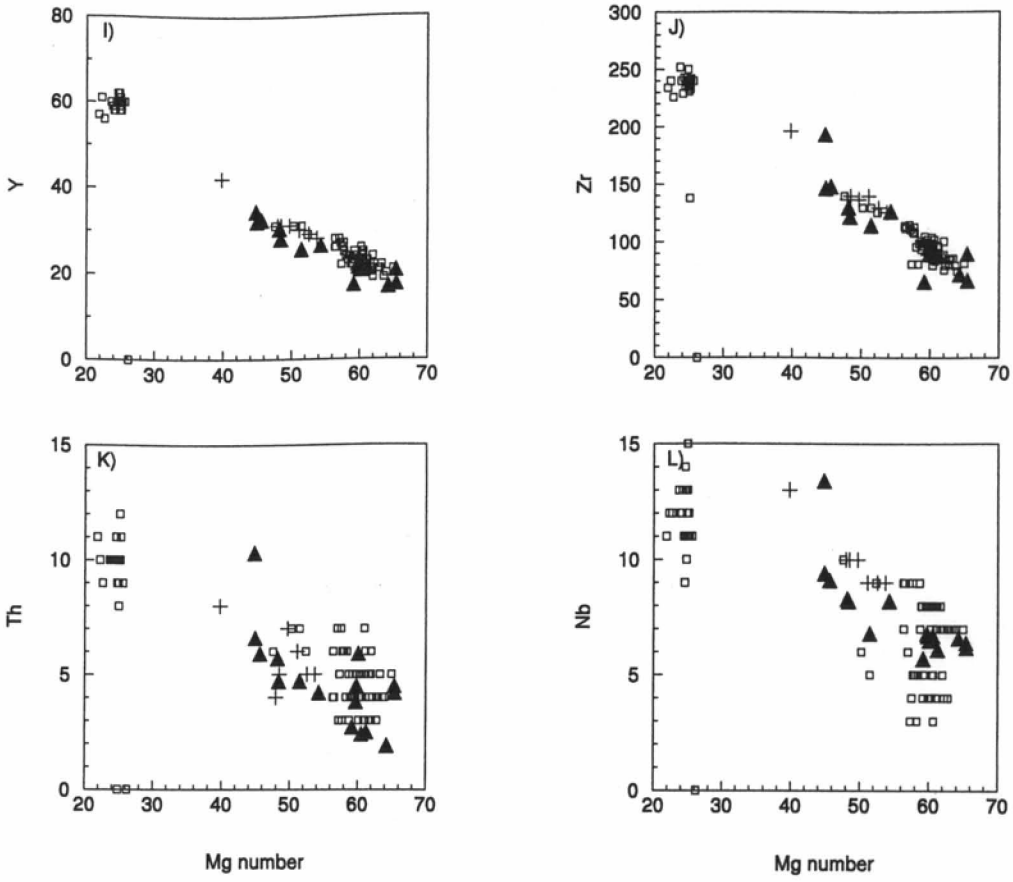

Fig. 6. (continued)

high SiO_2 and K_2O, and low FeO, CaO, and MgO. The mobile LIL elements (Ba, Rb, and Pb) and the HFS incompatible elements (Th, Zr, and Nb) are also high whereas V is low.

VII. Discussion

The new data for the CTM sills correlate with previous results obtained for Ferrar intrusive and extrusive rocks in Victoria Land. The sills exhibit the same major and trace element chemical signatures as the MFCT lavas. The chemical trends exhibited by the MFCT lavas and sills indicate they share the same source, and indicate that the magmas evolved primarily by fractional crystallization. None of the sills analyzed have the SPCT composition or are high MgO (MgO=8-9%) dolerites. The geochemistry, indicating only MFCT compositions and none that is distinctive, prevents addressing questions of supra-crustal transport. However, by expanding the database of the sills into the CTM, the research confirms that the Ferrar is composed of essentially one magma type derived from a single source (Fleming et al., 1997), and emplaced over a distance of more than 3000 km. This makes the FLIP unique in terms of other flood basalt provinces (Parana, Karoo, Columbia River), which are composed of multiple magma types (respectively: Peate, 1997; Marsh et al., 1997; Hooper, 1997). This work also sampled sills higher in the stratigraphic column than the previous work (Hamilton, 1965;Gunn, 1966) that concentrated on sills in the basement rock and Taylor Group. This is significant since the described olivine-bearing dolerite sills are emplaced low in the stratigraphic column. In CTM, the Kirkpatrick Basalt lavas are strongly evolved (almost all have MgO<4%), and differences in regional geochemistry have been used to suggest major centers of magmatism (Elliot & Fleming, in press). The sills do not show a comparable pattern, all but one having MgO>4%, and thus do not support the inferred regional pattern.

One sill (96-64-9) differs from the rest in a number of major and trace element abundances. A poor analysis seems improbable because the rock is different from the rest of the sill samples in thin section (see petrography). *In situ* differentiation could also produce results that do not correlate with observed trends. This occurs often in thick sills of the Ferrar Group, forming bodies of dolerite pegmatite and granophyre (Hamilton, 1965; Gunn, 1966). However, the sample was collected from the more rapidly cooled, chilled margin of a sill; the chilled margin normally records the magma composition, and eliminates the probability of *in situ* differentiation affecting the analysis. The sill could be a liquid formed during differentiation of a massive body, and later injected into adjacent country rock, in this case the Prebble Formation. This hypothesis is supported by the petrography and chemistry of the sample. The low CaO and MgO can be attributed to the small amount of calcic plagioclase and Mg-rich pyroxene, both of which would crystallize out in the early stages of evolution. The high K abundances are consistent with late stage alkali-rich feldspar crystallization, which is likely in granophyric intergrowths. The LIL elements substitute for K in the late stages of magma evolution, and, therefore, are also expected to be present in the alkali-feldspar in the granophyric intergrowth. FeO and V are present in magnetite and the low abundances for both of these components may be attributed to the relatively small amount of opaques in the rock. High fluid content, inferred from the elongate plagioclase and opaques, also indicate a differentiated melt. Furthermore, the field geology lends some support to this hypothesis. Near the location of this sill, a thick granophyre crops out which indicates a massive body below (D.H. Elliot, pers. comm. 2003). A large amount of magma is needed to produce a relatively small

amount of differentiated liquid; expulsion of this liquid into the country rock and its crystallization might explain this atypical sample.

VIII. Conclusion

The chemistry of the sills in the Shackleton Glacier region all lie on the MFCT trend, except for one that is interpreted to be a liquid differentiate of a large magma body, which was injected into country rock to form a sill. The chemical trends exhibited by these MFCT sills indicate they share the same source as other MFCT lavas and sills, and indicate that the magmas evolved primarily by fractional crystallization. The sills do not reflect the geographical pattern of chemistry noted for the lavas. The homogeneity of the Ferrar Group over vast distances (3000+ km) makes it unique compared with other flood basalt provinces. This research contributes to the present geochemical database of the Ferrar Group; better understanding of its emplacement and mode of transport may be obtained by enlarging the geographic coverage of geochemical data, and selection of samples for isotopic analysis.

References

Brewer, T.S., Hergt, J.M., Hawkesworth, C.J., Rex, D. and Storey, B.C. (1992) Coats Land dolerites and the generation of Antarctic continental flood basalts. In: Storey, B.C., King, E.C. and Livermore, R.A. (Eds.), Magmatism and the Causes of Continental Break-up. Geol. Soc. London, Spec. Publ., v. 68, pp. 185-208.

Brotzu, P., Capaldi, G., Civetta, L., Orsi, G., Gallo, G. and Melluso, L. (1992) Geochronology and Geochemistry of Ferrar rocks from north Victoria Land, Antarctica, Eur. J. Mineral., v. 4, pp. 605-617.

Collinson, J.W., Isbell, J.L., Elliot, D.H., Miller ,M.F. and Miller, J.M.G. (1994) Permian-Triassic Transantarctic Basin. In: Veevers, J. J. and Powell, C.McA. (Eds.), Permian-Triassic Pangean Basins and Foldbelts Along the Panthalassan Margin of Gondwanaland. Geol. Soc. Amer., Mem. 184, Boulder, Colorado, pp. 173-222.

Compston, W., McDougall, I. and Heier, K.S. (1968) Geochemical comparison of the Mesozoic basaltic rocks of Antarctica, South Africa, South America and Tasmania. Geochim. Cosmochim. Acta., v. 32, pp. 129-149.

Elliot, D.H. (1970) Jurassic tholeiites of the central Transantarctic Mountains, Antarctica. In: Gilmour, E.H. and Stradling, D. (Eds.), Proc. of the Second Columbia River Basalt Symposium. Cheney, Washington, March 1969, pp. 301-325.

Elliot, D.H. (1996) The Hanson Formation: a new stratigraphical unit in the Transantarctic Mountains, Antarctica. Antarctic Science, v. 8, pp. 389-394.

Elliot, D.H. (2000) Stratigraphy of Jurassic pyroclastic rocks in the Transantarctic Mountains. Journal of African Earth Sciences, v. 31, pp. 77-89.

Elliot, D.H. and Larsen, D. (1993) Mesozoic volcanism in the Transantarctic Mountains: depositional environments and tectonic settings, In: Findlay, R.H., Unrug, R., Banks, H.R. and Veevers, J.J. (Eds), Gondwana 8: Assembly, Evolution, and Dispersal. A.A. Balkema, Rotterdam, pp. 397-410.

Elliot, D.H. and Fleming, T.H. (in press) Occurrence and dispersal of magmas in the Jurassic Ferrar Large Igneous Province, Antarctica. Gondwana Research.

Elliot, D.H., Fleming, T.H., Haban, M.A. and Siders, M.A. (1995) Petrology and mineralogy of the Kirkpatrcik Basalt and Ferrar Dolerite, Meas Range region, north Victoria Land, Antarctica. In: Elliot, D.H. and Blaisdell, G.L. (Eds.), Contributions to Antarctic Research IV. Antarctic Research Series, v. 67, pp. 103-141.

Elliot, D.H., Fleming, T.H., Kyle, P.R. and Foland, K.A. (1999) Long distance transport of magmas in the Jurassic Ferrar Large Igneous Province, Antarctica. Earth Planet. Sci. Lett., v. 167, pp. 67-104.

Faure, G., Pace, K.K. and Elliot, D.H. (1982) Systematic variations of $^{87}Sr/^{86}Sr$ and major element concentrations in the Kirkpatrick Basalt of Mount Falla, Queen Alexandra Range, Transantarctic Mountains. In: Craddock, C. (Eds.) Antarctic Geoscience. University of Wisconsin Press, Madison, Wisconsin, pp. 715-723.

Fleming, T.H., Elliot, D.H., Jones, L.M., Bowman, J.R. and Siders, M.A. (1992) Chemical and isotopic variations in an iron-rich lava flow from the Kirkpatrick Basalt, north Victoria Land, Antarctica: implications for low-temperature alteration. Contrib. Mineral. Petrol., v. 111, pp. 440-457.

Fleming, T.H., Foland, K.A. and Elliot, D.H. (1995) Isotopic and chemical constraints on the crustal evolution and source signature of Ferrar magmas, north Victoria Land, Antarctica. Contrib. Mineral. Petrol., v. 121, pp. 217-236.

Fleming, T.H., Heimann, A., Foland, K.A. and Elliot, D.H. (1997) $^{40}Ar/^{39}Ar$ geochronology of Ferrar Dolerite sills from the Transantarctic Mountains, Antarctica: Implications for the age and origin of the Ferrar magmatic province. Geol. Soc. Amer. Bull., v. 109, pp. 533-546.

Fleming, T.H., Foland, K.A. and Elliot, D.H. (1999) Apophyllite $^{40}Ar/^{39}Ar$ and Rb-Sr geochronology: Potential utility and application to the timing of secondary mineralization of the Kirkpatrick Basalt, Antarctica. Journal of Geophysical Research, v. 104, pp. 20,081-20,095.

Gunn, B.M. (1966) Modal and element variationin Antarctic tholeiites. Geochim. Cosmochim. Acta, v. 30, pp. 881-920.

Haban, M.A. (1984) Mineral chemistry and petrogenesis of the Ferrar Supergroup, north Victoria Land, Antarctica (unpublished). MS thesis, pp. 161, Ohio State Univ, Columbus, Ohio.

Hamilton, W. (1965) Diabase sheets of the Taylor Glacier region Victoria Land, Antarctica. U.S. Geol. Sur. Prof. Pap., v. 456-B, pp. 1-71.

Heimann, A., Fleming, T.H., Elliot, D.H. and Foland, K.A. (1994) A short interval of Jurassic flood basalt volcanism in Antarctica as demonstrated by $^{40}Ar/^{39}Ar$ geochronology. Earth Planet. Sci. Lett., v. 121, pp. 19-41.

Hergt, J.M., Chappell, B.W., McCulloch, T.M., McDougall, I. and Chivas, A.R. (1989) Geochemical and isotopic constraints on the origin of the Jurassic dolerites of Tasmania. J. Petrol., v. 30, pp. 841-883.

Hoefs, J., Faure, G. and Elliot, D.H. (1980) Correlation of ^{18}O and initial $^{87}Sr/^{86}Sr$ ratios in Kirkpatrick Basalt on Mt. Falla, Transantarctic Mountains. Contrib. Mineral. Petrol., v. 75, pp. 199-203.

Hooper, P.R. (1997) The Columbia River Flood Basalt Province: Current status. In: Mahoney, J.J. and Coffin, M.F. (Eds.), Large Igneous Provinces: Continental, Oceanic, and Planetary Flood Volcanism. Geophysical Monograph v. 100, pp. 1-28.

Kyle, P.R. (1980)Development of heterogeneities in the subcontinental mantle: evidence from the Ferrar Group, Antarctica. Contrib. Mineral. Petrol., v. 73, pp. 89-104.

Kyle, P.R., Pankhurst, R.J. and Bowman, J.R. (1983) Isotopic and chemical variation in Kirkpatrick Basaltgroup rocks from southern Victoria Land. In: Oliver, R.L., James, P.R. and Jago, J.B. (Eds.), Antarctic Earth Science, Australian Academy of Science, Canberra, pp. 234-237.

Leat, P.T., Luttinen, A.V., Storey, B.C. and Millar, I.L. (in press) Sills of the Theron Mountains, Antarctica: more evidence for long distance transport of mafic magmas during Gondwana breakup. Proceedings of the 4th International Dyke Conference.

Marsh, J.S., Hooper, P.R., Rehacek, J., Duncan, R.A. and Duncan, A.R. (1997) Stratigraphy and age of Karoo Basalts of Losotho and implications for correlations within the Karoo Igneous Province. In: Mahoney, J.J. and Coffin, M.F. (Eds.), Large Igneous Provinces: Continental, Oceanic, and Planetary Flood Volcanism. Geophysical Monograph v. 100, pp. 247-272.

Peate, D.W. (1997) The Parana-Etendeka Province. In: Mahoney, J.J. and Coffin, M.F. (Eds.), Large Igneous Provinces: Continental, Oceanic, and Planetary Flood Volcanism. Geophysical Monograph v. 100, pp. 217-246.

Siders, M.A. and Elliot, D.H. (1985) Major and trace element geochemistry of the Kirkpatrick Basalt, Mesa Range, Antarctica. Earth Planet. Sci. Lett., v. 72, pp. 54-64.

Appendix

Petrography

96-50-5 Thanksgiving Point. Plagioclase and pyroxene occur in an intergranular texture. Plagioclase forms subhedral to euhedral crystals that usually show Albite twins and less commonly Carlsbad-Albite twins. The crystals are lathe shaped and up to 2 mm in length. The clinopyroxene is heavily altered to an orange-brown phyllosilicate with both augite and pigeonite phases. The two phases appear identical and can only be differentiated by their optic axial angles (2V). The clinopyroxene is anhedral to subhedral and up to 1 mm. Anhedral quartz crystals are also present that are less then 1 mm. Anhedral to subhedral opaques are disseminated throughout and are less then 0.5 mm.

96-51-18 Sill 1, Rougier Hill. Plagioclase and clinopyroxene occur in a subophitic texture. Plagioclase has a composition of An_{54} and forms subhedral to euhedral laths that are commonly 2.0-2.5 mm, but can reach 4 mm. Plagioclase commonly displays Albite twins with Carlsbad-Albite twins being less common and rare pericline twins. Plagioclase is altered slightly to an orange-brown phyllosilicate. Subhedral crystals of clinopyroxene range from 0.25-2 mm with some displaying simple twins. Augite is the dominant phase with pigeonite being less common. The two phases appear identical and can only be differentiated by their optic axial angles (2V). The clinopyroxene shows alteration to a fibrous light brown mineral interpreted to be tremolite/actinolite, but the crystals are too small for positive identification. Subhedral crystals of orthopyroxene are also present in small amounts, and range from 0.5-1.5 mm. The orthopyroxene appears identical to the clinopyroxene and can only be identified by a negative axial sign. Anhedral to subhedral sanidine crystals range from 0.5-3 mm. Quartz forms anhedral crystals from 0.5-1.5 mm. Quartzofeldspathic intergrowths form a granophyric texture. Subhedral crystals of biotite up to 2 mm are present. Apatite forms euhedral crystals that are usually less then 0.1 mm, but can reach up to 0.5 mm. Opaques are anhedral to subhedral and are less then 1 mm.

96-51-41 Sill 2, Rougier Hill. Plagioclase and clinopyroxene occur in a subophitic texture. Plagioclase forms twinned subhedral to euhedral laths up to 7 mm with some bent crystals arising from rapid cooling. Plagioclase commonly shows Albite twins and to a lesser extent Carlsbad-Albite twins. Subhedral to anhedral clinopyroxene crystals up to 4 mm are present. Augite is the dominant phase with pigeonite being less common. The two phases appear identical and can only be differentiated by their distinct optic axial angles (2V). The clinopyroxene shows heavy alteration to a fibrous light brown mineral interpreted to be tremolite/actinolite. Quartz forms anhedral crystals up to 2.5 mm. Quartzofeldspathic intergrowths form a granophyric texture that is being replaced by a brown-orange phyllosilicate. Euhedral and occasionally subhedral crystals of apatite commonly are less then 0.5 mm. Opaques are up to 1.5 mm and are anhedral to subhedral with most being skeletal from rapid cooling.

96-51-42 Sill 3, Rougier Hill. Plagioclase and clinopyroxene occur in an intergranular texture. Twinned subhedral to euhedral laths of plagioclase up to 7 mm are present. There are also thin wisp like crystals of plagioclase crystals in the mesostasis and bent plagioclase indicating rapid cooling. The plagioclase are commonly twinned along the Albite Law and less commonly twinned along the Carlsbad-Albite Law. The composition of the plagioclase is An_{50}, and it is altered to a light orange phyllosilicate. Clinopyroxene forms subhedral to anhedral crystals that are up to 2 mm. Augite is the dominant phase with pigeonite being rare. The two phases appear identical and can only be differentiated by their distinct optic axial angles (2V). The clinopyroxene shows slight alteration to a fibrous light brown mineral interpreted to be tremolite/actinolite. Anhedral quartz crystals are up to 1 mm. Quartzofeldspathic mesostasis forms a granophyric texture. Opaques are disseminated throughout and less then 0.1 mm.

96-51-72 Sill 4, Rougier Hill. Plagioclase and clinopyroxene occur in a subophitic texture. Plagioclase forms elongate laths that occasionally are zoned. The crystals are subhedral to euhedral and are up to 1.5 mm in length. Twinning is common along the Albite Law and less common along the Carlsbad-Albite Law. Subhedral clinopyroxene crystals are up to 2 mm. Augite and pigeonite are both found, but augite is the dominant phase. The two phases appear identical and can only be differentiated by their distinct optic axial angles (2V). The clinopyroxene shows alteration to a fibrous light brown mineral interpreted to be tremolite/actinolite, but too small for positive identification. Quartz forms anhedral grains up to 2 mm, and

encloses small clinopyroxene grains. Quartzofeldspathic mesostasis forms a granophyric texture. Opaques vary from anhedral to subhedral and are less then 0.5 mm.

96-51-76 Sill 5, Rougier Hill. Plagioclase and clinopyroxene occur in an intergranular texture. Plagioclase is An_{50} and forms elongate euhedral laths up to 7 mm. The plagioclase is usually twinned by the Albite Law with Carlsbad-Albite twins occurring less, and some of the plagioclase is bent indicating rapid cooling. Clinopyroxene display simple twins, is anhedral to subhedral, and up to 2.5 mm. Augite and pigeonite are the two phases with augite being dominant. Pigeonite is observed exsolving augite. The two are indistinguishable visually and alter to fine brown needles that are interpreted to be tremolite/actinolite. The two can only be distinguished by their optic axial angles (2V). Subhedral orthopyroxene xenocrysts are up to 8 mm. A gold-brown reaction rim surrounds the orthopyroxene. Quartz forms anhedral crystals that are 1 mm. Euhedral elongate needles of apatite are less then 0.5 mm. Quartzofeldspathic mesostasis forms a granophyric texture. Opaques are anhedral to euhedral crystals up to 1mm with some forming elongate needles.

96-57-4 East, Otway Massif. Plagioclase and clinopyroxene occur in an intergranular texture. Plagioclase forms elongate euhedral laths up to 2.5 mm that are frequently zoned. The plagioclase are commonly twinned along the Albite Law and less commonly twinned along the Carlsbad-Albite Law. Plagioclase is altering in places to a red-brown to black phyllosilicate. Anhedral to subhedral clinopyroxene crystals up to 3 mm are present. The clinopyroxene is altered to a brown fibrous mineral and displays two distinct degrees of alteration from low to high. The highly altered variety can not be identified optically, and the slightly altered variety is pigeonite. The highly altered variety could be a different pyroxene (augite?). Anhedral quartz crystals are up to 1.5 mm. Quartzofeldspathic mesostasis forms a granophyric texture. Opaques are anhedral to euhedral with elongate variety up to 3 mm.

96-64-1 West, Otway Massif. Plagioclase and clinopyroxene occur in a subophitic texture in a hypocrystalline matrix. Plagioclase forms euhedral elongate laths up to 6 mm that are commonly zoned with a composition of An_{64}. Small wisp like crystals of plagioclase also occurs in the glassy matrix that indicates rapid cooling. Albite twins are the most common with Carlsbad-Albite twins secondary. Subhedral clinopyroxene crystals up to 7.5 mm commonly form simple twins. Augite and pigeonite are the two phases present and they occur in roughly equal amounts. Augite infrequently rims the pigeonite. The two phases are only distinguishable by their optic axial angles (2V). The glass is slightly altered to a yellow mineraloid (palagonite). Apatite forms euhedral elongate needles that are less then 0.5 mm. Opaques range from anhedral to euhedral and are up to 3 mm.

96-64-9 West, Otway Massif. Plagioclase and clinopyroxene occur in a quartzofeldspathic rich matrix. Subhedral elongate laths of plagioclase are up to 6 mm. Plagioclase twinning is uncommon due to alteration. Clinopyroxene forms anhedral to subhedral crystals that range from 0.5 to 2 mm. Augite and pigeonite are the two phases present with augite being the dominant. The two types can not be distinguished visibly, and can only be differentiated using the optic axial angles (2V). Anhedral crystals of quartz are present that are up to 2 mm. Quartzofeldspathic intergrowth forms abundant granophyric texture. Apatite occurs as euhedral crystals that are less than 2 mm. Anhedral to euhedral opaque crystals up to 2 mm are present with some forming elongate laths, needles and hexagonal shapes.

96-64-13 West, Otway Massif. Plagioclase and clinopyroxene occur in subophitic texture. Plagioclase forms euhedral elongate laths that have a composition of An_{54} with some crystals being zoned. The crystals are up to 10 mm, but the majority are less than 5 mm. The plagioclase are commonly twinned along the Albite Law and less commonly twinned along the Carlsbad-Albite Law. Clinopyroxene is subhedral with some having simple twins. The clinopyroxene crystals are up to 12.5 mm with the majority being less than 6 mm. There are two phases present, augite and pigeonite, with augite being dominant, and some augite crystals are exsolving pigeonite. The two types can not be distinguished visibly, and can only be differentiated using the optic axial angles (2V). Clinopyroxene is slightly altered to a brown fibrous mineral (tremolite/actinolite). Quartz is anhedral and is smaller then 1.5 mm. Quartzofeldspathic intergrowth forms granophyric texture. The mesostasis is altered to an orange brown phyllosilicate. Apatite forms euhedral crystals that are less than 0.5 mm. Anhedral to subhedral opaques form crystals that are up to 6 mm with most being much smaller.

96-64-14 West, Otway Massif. Plagioclase and clinopyroxene occur in an intersertal to intergranular texture. Plagioclase forms subhedral to euhedral laths that are up to 5 mm. When enclosed in glass the plagioclase forms skeletal crystals and thin wisps that are the result of quenching. Albite and Carlsbad-Albite twinning is present but is not well developed, and some crystals are zoned. Anhedral to subhedral clinopyroxene crystals are up to 14 mm, but are usually less then 4 mm. Augite and pigeonite phases are present with augite being dominant. The two types can not be distinguished visibly, and can only be differentiated using the optic axial angles (2V). Simple twinning is common, and the clinopyroxene forms very small crystals that form trains in the glass. Skeletal opaques are also present in the glass, and are up to 1mm. The sample is unaltered except for a yellow mineraloid (palagonite) present in the glass.

96-73-6 Sill #1, Bennett Platform. Plagioclase and pyroxene occur in an intergranular texture. Elongate subhedral to euhedral laths of plagioclase are up to 4 mm. Twinning is along the Albite Law and less commonly along Carlsbad-Albite Law. Both clinopyroxene and orthopyroxene are present with orthopyroxene occurring infrequently. Augite is the clinopyroxene phase present and forms subhedral crystals up to 2 mm. The augite is altered to a fibrous brown mineral interpreted to be tremolite/actinolite. The orthopyroxene is not altered and forms subhedral crystals that are up to 2 mm. Anhedral crystals of quartz are up to 2.5 mm. Apatite forms euhedral needles that are less then 0.5 mm. Opaques are anhedral to euhedral and are less then 0.5 mm. A red brown phyllosilicate is also present and appears to be from alteration.

96-73-10 Sill #2, Bennett Platform. Plagioclase and pyroxene occur in an intergranular texture. Plagioclase is subhedral to euhedral, and up to 3 mm in length. It is commonly twinned along the Albite Law and less commonly along the Carlsbad-Albite Law. The pyroxene is highly altered to brown fibrous mineral (tremolite/actinolite?) making identification of the types present very difficult. Augite has been positively identified using the optic axial angle (2V). The crystals are up to 3 mm and are anhedral to subhedral. Quartz crystals are anhedral and up to 1 mm. Euhedral apatite needles are present that are less then 0.1 mm. Disseminated opaques, anhedral-subhedral, occur throughout the sample with some elongate rods that are less then 0.5 mm.

96-73-16 Sill #3, Bennett Platform. Plagioclase and clinopyroxene occur in an intergranular texture. Plagioclase, subhedral, is up to 4 mm in length and both Albite and Carlsbad-Albite twins are present, but not well developed due to alteration. Augite and pigeonite are the clinopyroxene phases present and are distinguished by their optic axial angles (2V). Simple twinning is present and crystals are up to 8 mm with most less than 3 mm. Disseminated opaques, up to 0.5 mm, occur throughout the section, and are anhedral to subhedral. The sample is highly altered to an orange-brown phyllosilicate.

96-74-2 Upper Sill, Roberts Massif. Plagioclase and clinopyroxene occur in an intergranular texture. The entire sample is very fine grained, and has small dark material on the crystal rims and throughout the matrix making identification difficult. Plagioclase forms subhedral to euhedral laths that are up to 3 mm with most being less than 1 mm. Some of the plagioclase forms elongate needles too. Twinning is common along the Albite Law and Carlsbad-Albite twinning is not common. Both augite and pigeonite phases are present in the section, and can only be differentiated using the optic axial angles (2V). The crystals are anhedral to subhedral, and are up to 5 mm with most being less then 1 mm. Anhedral quartz crystals are present that are less then 1 mm. Quartzofeldspathic intergrowths form granophyric texture. Anhedral to euhedral opaques are disseminated throughout the section.

96-74-7 Lower Sill, Roberts Massif. Plagioclase and clinopyroxene occur in a subophitic texture. Plagioclase forms subhedral laths up to 3 mm that are commonly zoned. Twinning is along the Albite Law and less commonly the Carlsbad-Albite Law. Clinopyroxene forms both augite and pigeonite phases, which can be differentiated by color under uncrossed polars. The augite is light brown from tremolite/actinolite alteration, and the pigeonite is clear from not undergoing alteration. The augite also commonly rims the pigeonite. The crystals form large glomeroporphs with crystals up to 14 mm. Quartzofeldspathic intergrowths are present forming a granophyric texture. Long euhedral needles of apatite are up to 2.5 mm. Opaques are anhedral to euhedral crystals up to 3 mm. Skeletal opaques are present due to rapid cooling and some are needlelike.